UWB/INS Integrated Pedestrian Positioning for Robust Indoor Environments

Yuan Zhang, Xinglong Tan, and Changsheng Zhao

***Abstract*—Goal: Accurate robust ultra wideband (UWB) pedestrian indoor positioning becomes a challenging task when faced with robust indoor environments such as non-line of sight (NLOS) due to refraction of signals, multipath effect, etc. When the UWB system is faced with such a robust environment, its positioning accuracy is difficult to reach the centimeter level and the reliability of the system operation needs to be improved. In order to solve such problems, an ultra wideband/inertial navigation system (UWB/INS) integrated pedestrian navigation algorithm is proposed. On the one hand, UWB-based joint state estimation particle filtering is used for position calculation, and on the other hand, INS-based zero-speed update (ZUPT) algorithm is used for navigation information solution. Under the framework of the INS error equation, the navigation information fusion of the two systems is carried out. In the simple pedestrian environment, the average positioning accuracy of the UWB/INS algorithm is 53.8% higher than that of the UWB algorithm, 40% higher than the INS algorithm and 31% higher than Original UWB/INS algorithm. Under the robust pedestrian indoor positioning, the average positioning accuracy of the UWB/INS algorithm is 39.7% higher than that of the UWB algorithm, 37.5% higher than the INS algorithm and 53% higher than Original UWB/INS algorithm. The results of two sets of pedestrian indoor positioning experiments demonstrate the effectiveness of our approach.**

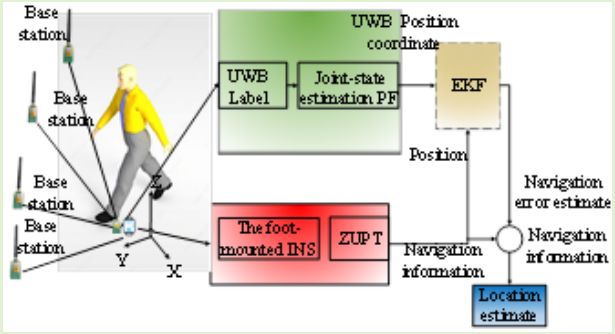

***Index Terms*—Pedestrian indoor positioning, UWB, INS, UWB/INS integrated navigation, NLOS.**

I. Introduction

With the rapid development of communication technology and the popularity of wireless networks, location services have become more and more concerned, and the application prospects are very broad such as indoor pedestrian navigation [1], [2], robot positioning [3], [4], drone positioning [5], [6], etc. According to the difference of the application scene, the positioning can be divided into indoor positioning and outdoor positioning. Outdoor positioning technologies such as the global positioning system (GPS) are widely visible in outdoor positioning scenes, but when faced with indoor environments, GPS does not provide the desired positioning effect. Indoor positioning technologies such as radio frequency identification (RFID), Zigbee, wireless local area network (WLAN), Bluetooth, etc. The accuracy of the above positioning method is in the meter level and cannot be adapted to the precision of high-precision pedestrian indoor navigation. UWB has the characteristics of strong penetrating ability and positioning accuracy of centimeter, which can meet the needs of high-precision pedestrian navigation. Current ranging methods based on different ranging methods can be divided into time of arrival (TOA) [7], received signal strength (RSS) [8], and time difference of arrival (TDOA) [9]. However, in a robust indoor environment, due to the object blocked by the wall or other signals, the signal transmission distance is increased and the transmission time is prolonged, resulting in a greatly reduced positioning accuracy. This phenomenon is called a NLOS case. In order to solve the NLOS problem in UWB ranging, many scholars have proposed some methods to deal with NLOS problem based on UWB ranging. However, most of the methods are based on data processing, often using the method of discarding NLOS information. For a single UWB system, even if some scholars put forward that considering the positive use of NLOS information, it can not adapt to robust indoor environment and ensure high precision indoor positioning. At present, the existing UWB positioning methods integrated with other methods such as INS, the accuracy is improved to some extent, but less positive consideration is given to the use of NLOS information. Therefore, for the robust NLOS indoor environment, the robust pedestrian integrated navigation and positioning algorithm needs to be put forward.

Manuscript received May 21, 2020; accepted May 27, 2020. Date of publication June 1, 2020; date of current version November 5, 2020. This work was supported in part by the Youth Fund Project of Jiangsu Natural Science Foundation under Grant BK20150236, in part by the Natural Science Fund of Jiangsu Normal University under Grant 15XLR019, and in part by the Jiangsu Postgraduate Innovation Project under Grant KYCX18_2161. The associate editor coordinating the review of this article and approving it for publication was Dr. Yen Kheng Tan. *(Corresponding author: Xinglong Tan.)*

The authors are with the School of Geography, Geomatics and Planning, Jiangsu Normal University, Xuzhou 221116, China (e-mail: 2020170726@jsnu.edu.cn; tanxinglong3@126.com; zhaocs1957@126.com).

Digital Object Identifier 10.1109/JSEN.2020.2998815

In the case of UWB ranging, NLOS environment will cause signal refraction and reflection, which will increase the transmission distance and the transmission time. This will increase the ranging error for distance measurement (such as TOA/TDOA). For the location methods based on distance measurement [10], [11], the authors want to use NLOS information and LOS information instead of discarding NLOS information, and use the joint vector of target motion state and target LOS/NLOS state to describe the target motion. A new joint state estimation particle filtering algorithm is proposed. This algorithm makes full use of NLOS information in robust environment, and can effectively improve the positioning accuracy to a certain extent. This algorithm provides a new way to deal with NLOS, but there are still some deviations in the results. Moreover, the disadvantage of this method is that a single system often needs to lay a large number of base stations, which may be expensive. For INS, this system has the characteristics of autonomous navigation, free from environmental constraints, and can be used for pedestrian-dominated navigation. Many pedestrian navigation algorithms based on INS have been proposed [12]–[16]. Aiming at foot-mounted INS system, the author studies the time period detection problem of ZUPT [12]. Estimating a person's position in a building is a necessary condition for creating intelligent space. The author describes and implements an INS-EKF-ZUPT framework based on Kalman filtering. By integrating foot-mounted IMU, the author proposes an open source, real-time and embedded implementation of foot- mounted, zero-speed updating aided INS [14]. However, the navigation error of INS based on low cost micro-electromechanical system (MEMS) accumulates over time, which can not provide long-term and high-precision navigation information. Many researchers have proposed various integrated navigation systems [15]–[18]. In order to maintain indoor horizontal accuracy during long-term indoor operation, the author proposes a system which combines ZUPT-assisted INS with RSS measurement. A real-time cooperative positioning system [16] is developed by using foot-bound low-cost inertial sensors and radio frequency-based ranging technology. Aiming at the influence of UWB non-line-of-sight error and drift error of INS inertial sensor, a tightly coupled UWB/INS system suitable for pedestrian room is proposed. Because the UWB signal is difficult to achieve large-scale interference coverage, the author proposes a GPS/INS/UWB integrated positioning scheme, and corrects its error to improve the positioning accuracy [18]. However, these algorithms are divided into UWB single system or INS single system, and integrated navigation system. In UWB single-system algorithm, too many base stations will make forgery expensive [19], [20]. In INS single-system algorithm, long-term tracking of the target will lead to drift and error accumulation phenomenon [21], [22]. In the integrated navigation algorithm, the NLOS situation in robust environment is seldom considered positively [22], [23].

On the basis of the existing joint state particle filter algorithm based on UWB, in order to achieve the positioning and navigation in the robust NLOS environment, we propose a new UWB/INS loose integrated pedestrian positioning method, which is realized by using UWB Mini4sPlus hardware and JY61 attitude sensor hardware. UWB positioning system uses UWB Mini4sPlus hardware to collect the distance data from the tag to the base station, and solves the position data of the tag through the joint state estimation particle filtering algorithm; INS positioning system uses JY61 attitude sensor hardware to collect acceleration and gyroscope 6-axis data, and calculates the navigation information of the target through ZUPT algorithm. UWB/INS integrated navigation adopts a loosely integrated method. The position information of the target pedestrian is independently calculated by UWB and INS. The INS error equation is used to fuse the position data of UWB and INS through Extended Kalman filter (EKF). For nonlinear problems, Kalman filtering is no longer applicable. The core idea of extended Kalman filtering is that for weakly nonlinear problems, the nonlinear function is expanded into Taylor series and the second-order and above terms are ignored to obtain an approximate linearized model. This can be processed using traditional Kalman filtering.

This paper consists of the following parts: Section II provides the location algorithm of LOS/NLOS joint state detection and UWB measurement. Section III presents the ZUPT algorithm based on foot-mounted IMU. Section IV presents the UWB/INS loosely integrated pedestrian positioning algorithm. Section V validates the algorithm on the hardware platform based on JY61 and UWB Mini4sPlus. Finally, the conclusion is drawn in Section VI.

II. Location Algorithm Based on LOS/NLOS Joint State Detection and UWB Measurement

A. Problem Description

We have laid M base stations with known coordinates in the area, and the target moves in the indoor area, and the distance data$y_t = \left(d_t^1, \ldots, d_t^M\right)$ between the target and the base station is obtained through the UWB Mini4sPlus hardware. Target motion state is defined as $(x_t, s_t)^T$, where $x = (X_{NT}, Y_{ET})$ represents the location of the target, where N and E represents North and East respectively, where $s_t = \left(s_t^1, \ldots, s_t^M\right)$ represents the LOS/NLOS status of different base stations. The sight state s_t^j is a binary variable with value $s_t^j = 1$ for LOS and $s_t^j = 0$ for NLOS conditions.

B. LOS/NLOS State Detection Method

The distance data is calculated by UWB Mini4sPlus hardware. In order to compensate UWB Mini4sPlus hardware system errors and take measurement noise into consideration. The distance d_t^j between the target and the j th base station at time t is measured as follows:

$$d_t^j = a \times \bar{d}_t^j + b + \upsilon_1 + \left(1 - s_t^j\right) \times \upsilon_2 \tag{1}$$

where $\bar{d}_t^j$ represents the real distance between the target and the jth base station; where a, b are the slope and intercept of the measured linear model, ideally the values are 1,0; υ_1 indicates measurement noise, which is zero mean Gaussian white noise; s_t^j represents LOS/NLOS status of the current time of the jth base station; υ_2 represents the noise caused by NLOS propagation, often a positive random number. In fact, a, b, and $\upsilon 1$ can be obtained through LOS measurement, while

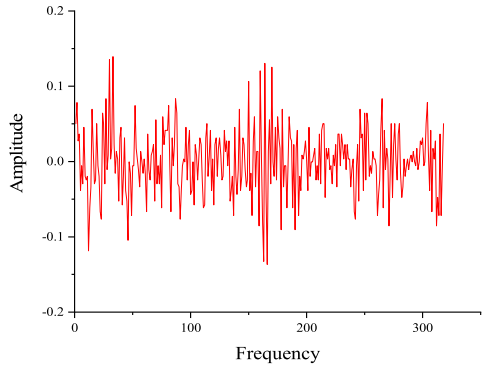

Fig. 1. Amplitude distribution of the measured noise v_1.

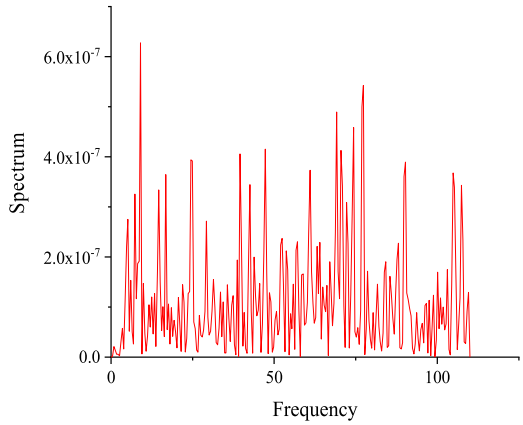

Fig. 2. Spectrum analysis of measurement noise v_1.

$v2$ is related to NLOS noise, which is relatively complicated and unknown.

Fig. 1 shows the amplitude distribution of the measured noise.UWB Mini4sPlus hardware is used to statically measure the distance data from the tag to the base station. After de-averaging, the amplitude distribution of the measured noise is obtained. It can be seen that the amplitude distribution is uniform.

Fig. 2 is a spectrum analysis diagram for measuring noise v_1. It can be seen that as the frequency changes, the spectrum distribution is uniform, and the measurement noise is excluded from the case of colored noise. Where v_1 is considered to be zero mean Gaussian white noise.

It can be seen from Fig. 3 that the LOS state measurement is substantially linear, while the NLOS measurement appears to be non-linear. Using the significant difference between LOS and NLOS, we can use the LOS measurement as an ideal measurement to determine whether the current measurement state is LOS or NLOS. The likelihood function p_t^j of the jth base station measured at time t is the LOS state is defined as:

$$p_t^j = \begin{cases} \frac{1}{\sqrt{2\pi}\sigma} \exp\left(-\frac{(d_t^j - \tilde{d}_t^j)^2}{2\sigma^2}\right) & if \quad \left(d_t^j > \tilde{d}_t^j\right) \\ 1 & else \end{cases} \tag{2}$$

where d_t^j represents distance data acquired by the jth base station, $\tilde{d}_t^j = a \times \bar{d}_t^j + b$ represents ideal distance measurement.

The first-order Markov process is used to describe the LOS/NLOS state of the base station, and the current time

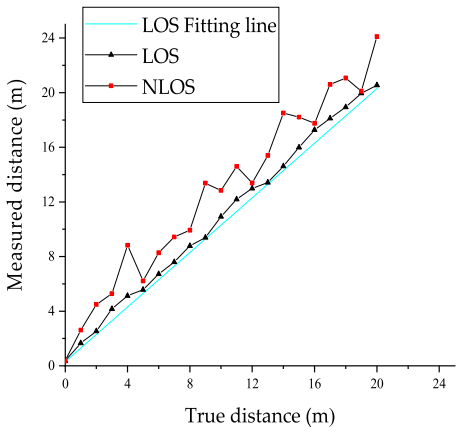

Fig. 3. Distance measurement under LOS/NLOS conditions.

state is estimated from the likelihood function of the current time and the state of the previous time. The LOS/NLOS state transfer function is defined as:

$$\begin{cases} p\left(s_t^j = 1 \middle| s_{t-1}^j = 1\right) = 0.9 \\ p\left(s_t^j = 0 \middle| s_{t-1}^j = 1\right) = 0.1 \\ p\left(s_t^j = 0 \middle| s_{t-1}^j = 0\right) = 0.9 \\ p\left(s_t^j = 1 \middle| s_{t-1}^j = 0\right) = 0.1 \end{cases} \tag{3}$$

Assuming that the LOS/NLOS states of the base stations are independent of each other, and the LOS/NLOS state at the previous moment is s_{t-1}^j, the current time state is:

$$s = \begin{cases} 1 & if \left(p\left(s_t^j = 1 \middle| s_{t-1}^j\right)\right) \times p_t^j > p_{threshold}) \\ 0 & else \end{cases} \tag{4}$$

where $p_{threshold}$ represents NLOS detection threshold.

C. Positioning Algorithm Based on LOS/NLOS Joint State Detection and UWB Measurement

1) State Model: Equation of state:

$$X(k) = \Phi X(k-1) + G\omega(k-1) \tag{5}$$

where Φ represents state transition matrix, G represents process noise drive matrix, $\omega(k)$ represents process noise. Target state vector is as follows:

$$X(k) = [X_N(k), Y_E(k), V_N(k), V_E(k)]^T \tag{6}$$

where we define the north and east directions as positive, $X_N(k)$ represents northward position, $Y_E(k)$ represents eastward position, $V_N(k)$ represents northward velocity, $V_E(k)$ represents eastward velocity.

2) Observation Likelihood Model: The positioning algorithm is essentially a particle filtering algorithm, and the joint state to be estimated is $(x_t, s_t)^T$. The LOS/NLOS state is obtained by equation (7). It can be seen from Fig. 3 that the NLOS distance measurement is always greater than the true distance, so the target must be in the center of the base station measured by NLOS, and within the circle of the NLOS measurement radius,

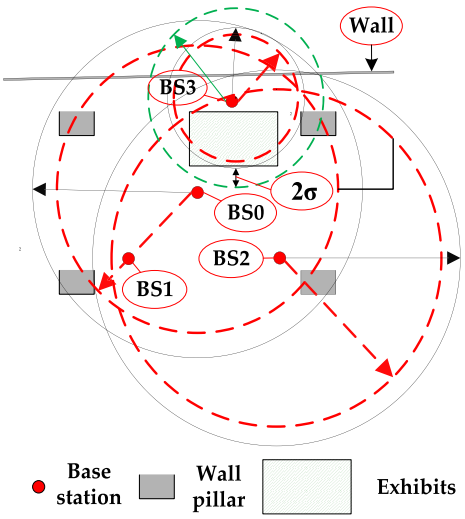

Fig. 4. Measurement scene in LOS/NLOS state.

if there are multiple NLOS measurements value, buildable target NLOS-based trusted area A is defined as follows:

$$A = \left\{ x \,|\, \|x - x_j\| \le d_t^j, j = 1, \ldots, K \right\} \tag{7}$$

here x_j represents the location of the jth base station, $\|x - x_j\|$ represents the distance from position x to the jth base station, and K is the number of currently detected NLOS measurements.

From Fig. 4, the feasible region is a little too big. To reduce the area of the feasible region, we build the enhanced feasible region by utilizing the LOS and NLOS measurements simultaneously, a trusted area B based on LOS information is constructed:

$$B = \left\{ x \,|\, \|x - x_j\| \le d_t^j + 2\sigma, j = 1, \ldots, L \right\} \tag{8}$$

where x_j is the location of the jth base station, $\|x - x_j\|$ is the distance from the position x to the jth base station, L is the number of currently detected LOS measurements, and σ is the measurement standard deviation. Therefore the enhanced trusted domain C is defined as:

$$C = A \cap B \tag{9}$$

The filtered particle filtering process is performed using the enhanced trusted domain C as follows:

$$\omega_{t-1}^i = \begin{cases} \omega_{t-1}^i & if \ \left(x_t^i \in \hat{\mathrm{E}}C\right) \\ 0 & else \end{cases} \tag{10}$$

For LOS measurement information, the observed likelihood function of the first particle is:

$$p\left(y_t \left| x_t^i \right.\right) = \left(\prod_{j=1}^{L} p_t^{ij} \right)^{1/L} \tag{11}$$

where L represents the total number of LOS measurements, and p_t^{ij} represents the probability that the ith particle acquires the observed d_t^j from the jth base station, as defined below:

$$p_t^{ij} = \frac{1}{\sqrt{2\pi}\sigma} \exp\left(-\frac{\left(d_t^j - \tilde{d}_t^{ij}\right)^2}{2\sigma^2} \right) \tag{12}$$

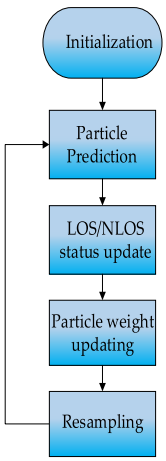

Fig. 5. Joint-state vector estimation process.

where $\tilde{d}_t^{ij} = a \times \bar{d}_t^{ij} + b$ represents ideal distance, $\bar{d}_t^{ij}$ represents the distance between particle i and jth base station.

The likelihood function of each particle is calculated by equation (10) and $\omega_{t-1}^i p\left(y_t \left| x_t^i \right.\right)$ will be used as the weight of each particle.

Fig. 5 gives a flow chart of the joint-state estimation algorithm. The framework of this algorithm is based on particle filtering, which is consistent with the basic processing of particle filtering. In the resampling phase, it is possible to judge whether or not to perform resampling based on the number of effective particles of the particle.

III. ZUPT Algorithm Based on Foot-Mounted IMU

For pedestrian autonomous navigation, the foot-mounted IMU is often implemented with a low-cost MEMS gyro and accelerometer. Due to the low precision of the MEMS device, the three errors of the position, velocity and attitude of the target are corrected by using the characteristics of the landing speed of zero to improve the accuracy of the autonomous navigation. The formula (13-15) given below refers to quotation [14], which is the key step of ZUPT solution. Continuous system discretization:

$$\begin{bmatrix} x_k \\ \upsilon_k \\ q_k \end{bmatrix} = \begin{bmatrix} x_{k-1} + \upsilon_{k-1} dt_k \\ \upsilon_{k-1} + \left(q_{k-1} f_k q_{k-1}^{-1} - g \right) dt_k \\ \Omega\left(\omega_k dt_k\right) q_{k-1} \end{bmatrix} \tag{13}$$

where dt_k represents the sampling interval, x_k represents the position, υ_k represents the speed, q_k represents the carrier system to the navigation coordinate system, f_k represents the acceleration measurement, g represents the gravity acceleration, ω_k represents the gyroscope measurement, and $\Omega(\cdot)$ represents the quaternion update matrix.

Kalman filtering correction process is as follows:

$$\begin{bmatrix} x_k \\ \upsilon_k \\ d\theta_k \end{bmatrix} = \begin{bmatrix} x_k \\ \upsilon_k \\ 0 \end{bmatrix} + K_k \upsilon_k \tag{14}$$

$$q_k \Leftarrow \Omega\left(d\theta_k\right) q_k \tag{15}$$

where K_k represents Kalman filtering gain matrix and $d\theta_k$ represents revised attitude angle.

Fig. 6 is a diagram of the ZUPT-aided INS algorithm. ZUPT assists the INS and obtains the position, velocity and

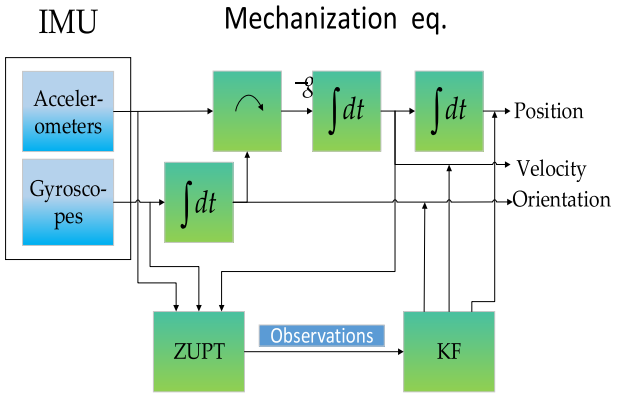

Fig. 6. Block diagram of the ZUPT-aided INS.

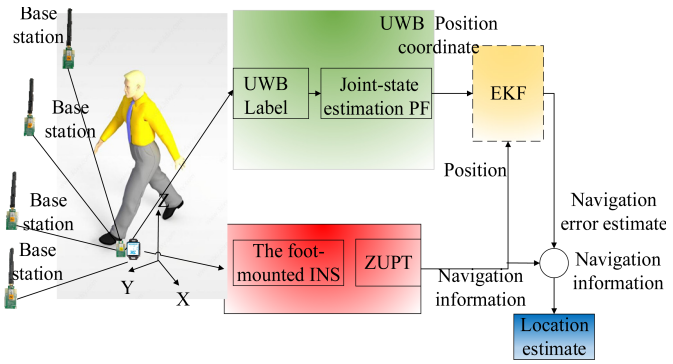

Fig. 7. Basic architecture of UWB/INS loose integrated navigation model.

attitude of the target through KF. On the one hand, the IMU with accelerometer and gyroscope can solve the velocity, position and attitude information of the target through the mechanized equation of the strapdown inertial navigation. On the other hand, the ZUPT algorithm can obtain the target accelerometer according to the foot-mounted IMU and the gyroscope information uses the characteristics of the landing speed of the target to measure the speed, as the observation, and updates the speed, position and attitude information of the target through Kalman filtering.

IV. UWB/INS Loosely Integrated System

A. The Basic Architecture of the Integrated Navigation Model

The basic architecture of UWB/INS loose integrated navigation is shown in Fig. 7. It mainly includes two parts: INS and UWB positioning system. Among them, the foot-mounted IMU (with accelerometer and gyroscope) is fixed to the pedestrian position, speed, attitude and other information through the ZUPT algorithm; the UWB positioning tag fixed on the pedestrian foot can obtain the distance from the tag to the base station. The position coordinates of the pedestrian are settled by a particle filtering algorithm based on the joint state estimation. On this basis, the extended Kalman filtering algorithm is used to fuse the coordinate data of the two positioning systems, and finally the error estimation of the INS navigation information and the settlement of the positioning coordinates are obtained.

B. System State Model

In UWB/INS integrated navigation, the strapdown inertial error equation is used as the system error equation and Kalman filtering is used for dynamic adjustment. The INS error equation is as follows [18]:

$$\delta\dot{r} = -\omega_{en} \times \delta r + \delta v \tag{16}$$

$$\delta\dot{v} = -(2\omega_{ie} + \omega_{en}) \times \delta v + \delta\psi \times f + \delta \tag{17}$$

$$\delta\dot{\psi} = -(2\omega_{ie} + \omega_{en}) \times \delta\psi + \varepsilon \tag{18}$$

where $\delta r, \delta v$ and $\delta\psi$ represent the position, velocity, and attitude misalignment angle error vectors, respectively, ω_{en} represents the angular rates of the navigation system relative to the Earth's coordinate system, and ω_{ie} represents the angular velocity of the Earth's coordinate system relative to the inertial system. δ represents the accelerometer zero offset error vector, ε represents the gyro drift error vector.

Considering equations (16)-(18), the system state can be expressed as:

$$\dot{X} = FX + GW \tag{19}$$

where X represents the error vector, F represents the state transition matrix, G represents the noise drive matrix, W represents the measurement noise.

C. Observation Model

For UWB/INS integrated navigation, the observation model consists of the coordinates of the UWB solution and the coordinate difference between the INS solutions:

$$Z = \begin{bmatrix} X_N^{UWB} - X_N^{INS} \\ Y_E^{UWB} - Y_E^{INS} \end{bmatrix} \tag{20}$$

The observation based on Kalman filtering is given:

$$Z_k = H_k X_k + \tau \tag{21}$$

where Z_k represents the observation vector, H_k represents the observation matrix, and τ represents the measurement noise, which is generally Gaussian noise.

Based on the state model and the observation model, Kalman filtering is used to fuse navigation information. Optimal estimation of Kalman filtering state vector by time update and measurement update.

V. Field Test and Analysis

A. Simple Experimental Environmental Inspection

In order to verify the performance of the above INS/UWB integrated algorithm in a simple environment, we did a simple experiment: there is no obvious NLOS situation in the environment, Walking counterclockwise along the rectangle 28.39m. In a simple indoor environment, the proposed UWB/INS integrated navigation algorithm is compared with the joint state estimation particle filter algorithm based on UWB, the INS algorithm based on ZUPT and Original UWB/INS(O-UWB/INS: Taking the inertial navigation error equation as the state equation and the position and velocity difference between the inertial navigation and UWB as the observation equations, the fusion is performed by EKF). The research contents include motion trajectory, cumulative distribution function of positioning errors, specific positioning errors at all times, etc. The performance parameters of various algorithms are analyzed. The IMU used in the test is a 6-axis attitude angle sensor as shown in Fig. 8. The UWB label used

Fig. 8. JY61 attitude angle sensor.

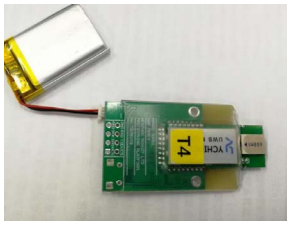

Fig. 9. UWB ranging label.

TABLE I
PERFORMANCE PARAMETERS OF JY61 ATTITUDE ANGLE SENSOR

Parameters	Gyroscope	Accelerometer
Initial bias error	±0.61 °	±0.0005 *g*
Random walk	18 °/*h*	±0.04 *mg*
Range	±2000 *deg/s*	±16 *g*

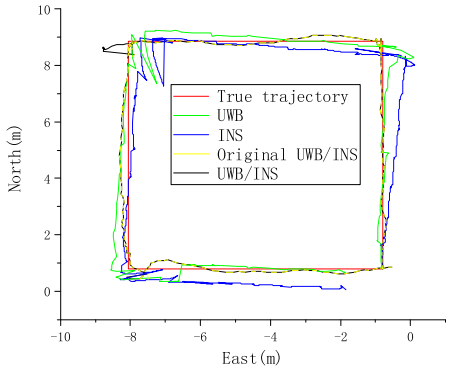

Fig. 10. Motion trajectory contrast in simple experimental environment.

is shown in Fig. 9 and the performance parameters of the IMU in the experiment are shown in TABLE I.

The default parameters of the integrated navigation algorithm are: $a = 1.0022, b = 0.3000, \sigma^2 = 1$, the number of particles is $N = 200$,and $p_{\text{Threshold}} = 0.005$.

Fig. 10 represents a comparison of the trajectories of various algorithms in a simple environment. It can be seen that all the algorithms can maintain good performance in the LOS environment.

Fig. 11 is a cumulative distribution function (CDF) of the positioning error, and Fig. 12 is a specific positioning error value at each time. TABLE II gives detailed error statistics for each algorithm, including mean, median, standard deviation, maximum, and position error in the east and north directions. The above results show that under the simple environment of LOS, all four algorithms can maintain better positioning results, and the proposed UWB/INS combined positioning algorithm can obtain better positioning effect, which can effectively improve the positioning accuracy.

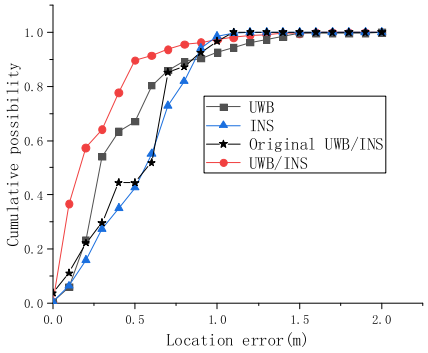

Fig. 11. CDF of localization error.

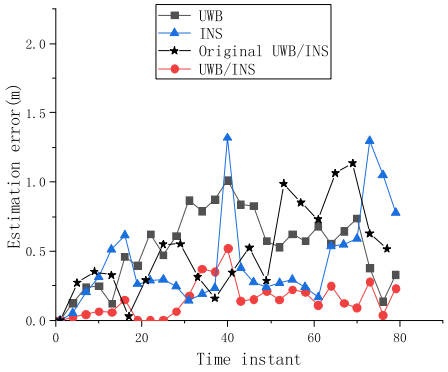

Fig. 12. Location error along the path.

TABLE II
COMPARISON OF LOCATION ERRORS OF FOUR ALGORITHMS IN A SIMPLE EXPERIMENTAL ENVIRONMENT

Algorithm	Mean(m)	Med(m)	Std(m)	Max(m)	N(m)	E(m)
UWB	0.52	0.55	0.26	1.12	0.41	0.41
INS	0.40	0.29	0.31	1.93	0.36	0.37
O-UWB/INS	0.35	0.39	0.27	1.72	0.44	0.32
UWB/INS	0.24	0.15	0.26	1.52	0.30	0.18

B. Robust Experimental Environmental Inspection

In order to analyze the performance of the above INS/UWB loosely integrated algorithm, the pedestrian positioning tracking test was conducted in the lobby of the first floor of Tianjia Bing Institute of Technology, Jiangsu Normal University. There is LOS/NLOS state in the scene map, which is called robust indoor environment. The test scene is shown in Fig. 13. The entire test area is $10.464m \times 13.670m$.The gray rectangular block represents the load-bearing column, the red point represents the base station, and the base station can be detected by the tag.

In the robust indoor environment, the proposed UWB/INS integrated navigation algorithm (UWB/INS) is compared with the UWB-based joint state estimation particle filtering algorithm, the ZUPT-based INS algorithm and Original UWB/INS algorithm. The performance parameters of various algorithms are analyzed.

Fig. 14, Fig. 16, Fig. 17 and Fig. 18 show the estimation results of the real trajectory with UWB, INS, Original UWB/INS and proposed UWB/INS combined algorithm respectively. Fig. 15 shows the LOS/NLOS state at each

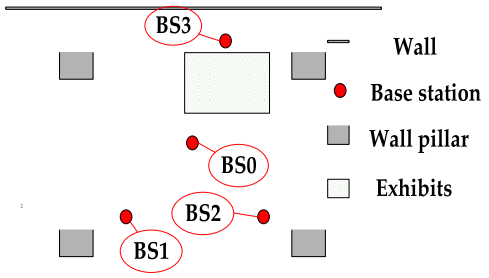

Fig. 13. Floor plan for the test bed.

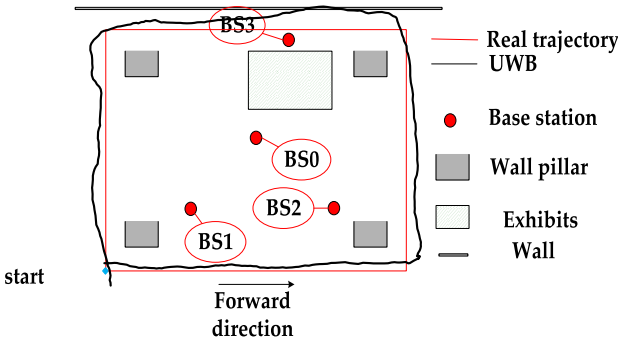

Fig. 14. UWB trajectory diagram.

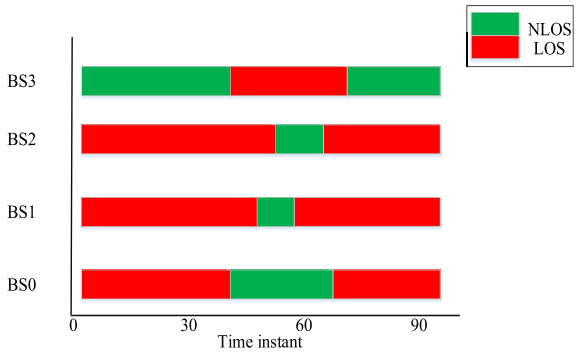

Fig. 15. Sight states along the path in UWB ranging environment.

time in UWB ranging environment. As is shown in Fig. 15, when pedestrians pass through a large occlusion, i.e. exhibits, the UWB algorithm can clearly recognize the NLOS status of pedestrians, but when pedestrians pass through a small occlusion with a load-bearing column, the algorithm can not clearly recognize the NLOS status of pedestrians. Fig. 14 is the trajectory of UWB algorithm. It can be found that there are some errors in UWB algorithm when passing through large exhibits, which corresponds to the LOS/NLOS state in Fig. 15. However, in Fig. 14, when pedestrians pass through small occlusions, i.e. load-bearing columns, the trajectory of UWB algorithm has a small deviation, which shows that UWB algorithm can't work with small occlusions. Identify the LOS/NLOS status of good travelers. By adding the INS algorithm, it can be seen that the UWB/INS integrated algorithm can obtain better estimation. In Fig. 17 and Fig. 18, we present the original UWB / INS and the trajectory of our proposed UWB / INS algorithm. From the comparison of Figures 17 and 18, the proposed UWB / INS algorithm is superior to the original UWB / INS algorithm. In this scenario, we mixed the NLOS and LOS environments for UWB.

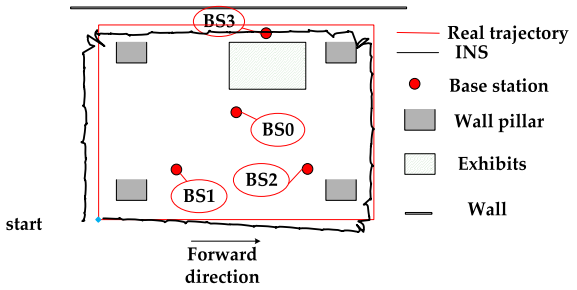

Fig. 16. INS trajectory diagram.

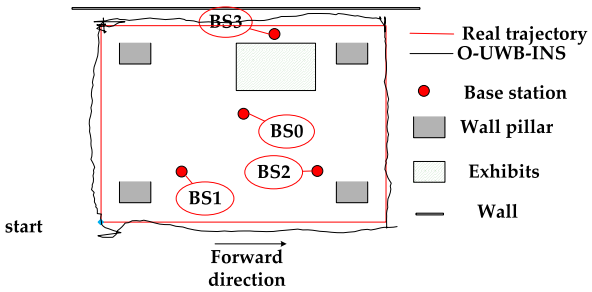

Fig. 17. Original UWB/INS (O- UWB/INS) trajectory diagram.

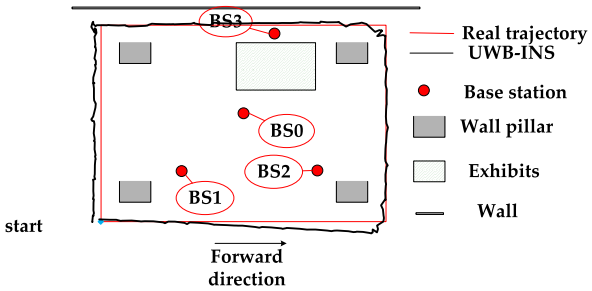

Fig. 18. UWB/INS trajectory diagram.

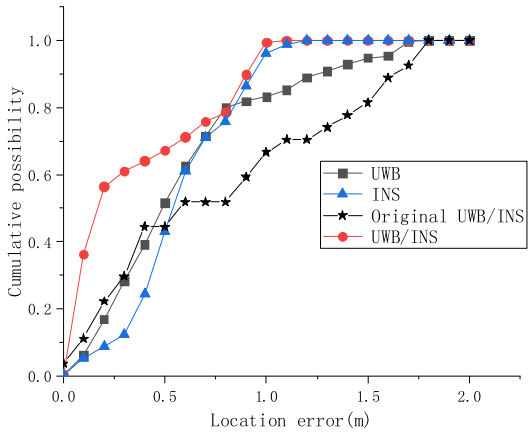

Fig. 19. CDF of localization error.

For the original UWB / INS algorithm, we can not consider the impact of this NLOS environment on the algorithm well. The proposed UWB / INS algorithm takes into account the NLOS environment. Therefore, it can be seen from the image that the proposed UWB / INS algorithm is superior to the original UWB / INS algorithm.

Fig. 19 is the cumulative distribution function (CDF) of positioning errors, and Fig. 19 is the specific value of

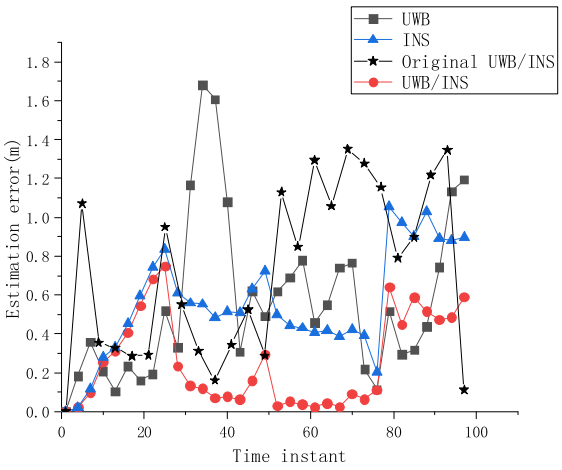

Fig. 20. Location error along the path.

TABLE III
COMPARISON OF LOCATION ERRORS OF THREE ALGORITHMS IN A ROBUST EXPERIMENTAL ENVIRONMENT

Algorithm	Mean(m)	Med(m)	Std(m)	Max(m)	N(m)	E(m)
UWB	0.58	0.49	0.42	1.72	0.63	0.34
INS	0.56	0.53	0.26	1.15	0.54	0.31
O-UWB/INS	0.74	0.61	0.59	1.76	0.51	0.79
UWB/INS	0.35	0.14	0.35	1.02	0.43	0.23

positioning errors at each time. We use UWB and INS loose combination, and this process is completed by extended Kalman filter. Before the program runs, we usually give the R matrix of measurement noise. This R matrix contains UWB measurement noise and INS measurement noise, and the selection of this value affects the final filtering results. As can be seen in Fig.20, the effect of UWB / INS combination is more favorable to INS in the period of 15-30 and 80-90. This shows that the UWB measurement noise is relatively large, while the ins measurement noise is relatively small, and the ins measurement noise plays a positive role. Therefore, the trajectory of UWB / INS combination is inclined to that of INS.TABLE III gives detailed error statistics of each algorithm, including mean, median, standard deviation, maximum and position errors in the East and North directions. The above results show that in the robust indoor environment, our proposed UWB/INS integrated navigation algorithm (UWB/INS) is better than the UWB-based joint state estimation particle filtering algorithm, ZUPT-based INS algorithm and the original UWB / INS algorithm.which can effectively improve the positioning accuracy. For robust indoor environments, it has better adaptability and robustness and can be used for pedestrian indoor navigation.

VI. CONCLUSIONS

Due to the existing joint state particle filter algorithm based on UWB ranging, although the NLOS information can be used positively, it can basically adapt to the robust pedestrian indoor environment, but there are problems such as insufficient positioning accuracy or unstable positioning. A new UWB/INS integrated navigation algorithm is proposed to track and locate pedestrian accurately in robust LOS/NLOS environment. UWB algorithm is based on joint state estimation particle filtering and INS algorithm is based on ZUPT algorithm. The algorithm uses UWB and INS loosely combined method. Each system solves the position of the target independently. The INS error is the state, and the coordinate difference between the two systems is the observation. The data fusion is carried out by extended Kalman filtering. Compared with the joint state particle filter single system algorithm based on UWB distance measurement, INS-based zero-speed update algorithm and Original UWB/ INS, the integrated navigation system of UWB/INS has higher accuracy and better adaptability. Based on UWB Minni4sPlus hardware and IMU JY61 hardware measurement team UWB/INS integrated algorithm, the performance of UWB/INS integrated pedestrian location algorithm is verified, and the accurate pedestrian tracking and pedestrian positioning in robust environment can be achieved.

REFERENCES

[1] L.-H. Chen, E. H.-K. Wu, M.-H. Jin, and G.-H. Chen, "Intelligent fusion of Wi-Fi and inertial sensor-based positioning systems for indoor pedestrian navigation," *IEEE Sensors J.*, vol. 14, no. 11, pp. 4034–4042, Nov. 2014.

[2] L. Pei, D. Liu, D. Zou, R. Lee Fook Choy, Y. Chen, and Z. He, "Optimal heading estimation based multidimensional particle filter for pedestrian indoor positioning," *IEEE Access*, vol. 6, pp. 49705–49720, 2018.

[3] H. Xie, T. Gu, X. Tao, H. Ye, and J. Lu, "A reliability-augmented particle filter for magnetic fingerprinting based indoor localization on smartphone," *IEEE Trans. Mobile Comput.*, vol. 15, no. 8, pp. 1877–1892, Aug. 2016.

[4] A. Amanatiadis, "A multisensor indoor localization system for biped robots operating in industrial environments," *IEEE Trans. Ind. Electron.*, vol. 63, no. 12, pp. 7597–7606, Dec. 2016.

[5] C. Luo, S. I. McClean, G. Parr, L. Teacy, and R. De Nardi, "UAV position estimation and collision avoidance using the extended Kalman filter," *IEEE Trans. Veh. Technol.*, vol. 62, no. 6, pp. 2749–2762, Jul. 2013.

[6] J.-J. Xiong and E.-H. Zheng, "Position and attitude tracking control for a quadrotor UAV," *ISA Trans.*, vol. 53, no. 3, pp. 725–731, May 2014.

[7] A. Moragrega, P. Closas, and C. Ibars, "Supermodular game for power control in TOA-based positioning," *IEEE Trans. Signal Process.*, vol. 61, no. 12, pp. 3246–3259, Jun. 2013.

[8] C. Feng, W. S. A. Au, S. Valaee, and Z. Tan, "Received-signal-strength-based indoor positioning using compressive sensing," *IEEE Trans. Mobile Comput.*, vol. 11, no. 12, pp. 1983–1993, Dec. 2012.

[9] S.-Y. Jung, S. Hann, and C.-S. Park, "TDOA-based optical wireless indoor localization using LED ceiling lamps," *IEEE Trans. Consum. Electron.*, vol. 57, no. 4, pp. 1592–1597, Nov. 2011.

[10] J. Wang, Q. Gao, Y. Yu, H. Wang, and M. Jin, "Toward robust indoor localization based on Bayesian filter using chirp-spread-spectrum ranging," *IEEE Trans. Ind. Electron.*, vol. 59, no. 3, pp. 1622–1629, Mar. 2012.

[11] W. Li and Y. Jia, "Location of mobile station with maneuvers using an IMM-based cubature Kalman filter," *IEEE Trans. Ind. Electron.*, vol. 59, no. 11, pp. 4338–4348, Nov. 2012.

[12] I. Skog, P. Handel, J.-O. Nilsson, and J. Rantakokko, "Zero-velocity detection—An algorithm evaluation," *IEEE Trans. Biomed. Eng.*, vol. 57, no. 11, pp. 2657–2666, Nov. 2010.

[13] A. R. Jimenez, F. Seco, J. C. Prieto, and J. Guevara, "Indoor pedestrian navigation using an INS/EKF framework for yaw drift reduction and a foot-mounted IMU," in *Proc. 7th Workshop Positioning, Navigat. Commun.*, Mar. 2010, pp. 135–143.

[14] J.-O. Nilsson, I. Skog, P. Handel, and K. V. S. Hari, "Foot-mounted INS for everybody—An open-source embedded implementation," in *Proc. IEEE/ION Position, Location Navigat. Symp.*, Apr. 2012, pp. 140–145.

[15] Q. Fan, B. Sun, Y. Sun, and X. Zhuang, "Performance enhancement of MEMS-based INS/UWB integration for indoor navigation applications," *IEEE Sensors J.*, vol. 17, no. 10, pp. 3116–3130, May 2017.

[16] J.-O. Nilsson, J. Rantakokko, P. Handel, I. Skog, M. Ohlsson, and K. V. S. Hari, "Accurate indoor positioning of firefighters using dual foot-mounted inertial sensors and inter-agent ranging," in *Proc. IEEE/ION Position, Location Navigat. Symp. (PLANS)*, May 2014, pp. 631–636.
[17] C. Ascher, L. Zwirello, T. Zwick, and G. Trommer, "Integrity monitoring for UWB/INS tightly coupled pedestrian indoor scenarios," in *Proc. Int. Conf. Indoor Positioning Indoor Navigat.*, Sep. 2011, pp. 1–6.
[18] Z. Li, R. Wang, J. Gao, and J. Wang, "An approach to improve the positioning performance of GPS/INS/UWB integrated system with two-step filter," *Remote Sens.*, vol. 10, no. 2, p. 19, Dec. 2017.
[19] Y. Luo and C. L. Law, "Indoor positioning using UWB-IR signals in the presence of dense multipath with path overlapping," *IEEE Trans. Wireless Commun.*, vol. 11, no. 10, pp. 3734–3743, Oct. 2012.
[20] L. Greenstein, S. Ghassemzadeh, S.-C. Hong, and V. Tarokh, "Comparison study of UWB indoor channel models," *IEEE Trans. Wireless Commun.*, vol. 6, no. 1, pp. 128–135, Jan. 2007.
[21] S. Cai, W. Liao, C. Luo, M. Li, X. Huang, and P. Li, "CRIL: An efficient online adaptive indoor localization system," *IEEE Trans. Veh. Technol.*, vol. 66, no. 5, pp. 4148–4160, May 2017.
[22] D. Simon Colomar, J.-O. Nilsson, and P. Handel, "Smoothing for ZUPT-aided INSs," in *Proc. Int. Conf. Indoor Positioning Indoor Navigat. (IPIN)*, Nov. 2012, pp. 1–5.
[23] A. Benini, A. Mancini, and S. Longhi, "An IMU/UWB/Vision-based extended Kalman filter for mini-UAV localization in indoor environment using 802.15.4a wireless sensor network," *J. Intell. Robotic Syst.*, vol. 70, nos. 1–4, pp. 461–476, Apr. 2013.
[24] S. Zihajehzadeh, P. K. Yoon, and E. J. Park, "A magnetometer-free indoor human localization based on loosely coupled IMU/UWB fusion," in *Proc. 37th Annu. Int. Conf. IEEE Eng. Med. Biol. Soc. (EMBC)*, Aug. 2015, pp. 3141–3144.

Yuan Zhang received the B.S. degree in surveying and mapping engineering from the Shandong University of Science and Technology, Qingdao, China, in 2017. He is currently pursuing the M.S. degree in geodesy and surveying engineering with Jiangsu Normal University.

His research interest includes UWB/INS integrated navigation.

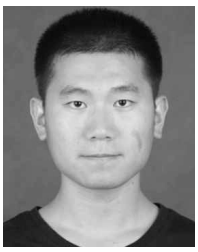

Xinglong Tan received the B.S. degree in mechanical engineering from the Nanjing University of Information Engineering, Nanjing, in 2008, and the M.S. and Ph.D. degrees in geodesy and surveying engineering from the China University of Mining and Technology, Xuzhou, China, in 2011 and 2014, respectively.

His research interests include GNSS/INS integrated navigation and indoor and outdoor seamless positioning.

Changsheng Zhao received the B.S. and M.S. degrees in geodesy and surveying engineering from the Liaoning University of Engineering and Technology, Fuxin, in 1982 and 1984, respectively, and the Ph.D. degree in geodesy and surveying engineering from Wuhan University, Wuhan, China, in 2008.

His research interests include geodetic survey and data processing.